P H Y S I C A L   R E V I E W   L E T T E R S

Influence of Polymer-Pore Interactions on Translocation

Kaifu Luo,[1],[*] Tapio Ala-Nissila,[1,2] See-Chen Ying,[2] and Aniket Bhattacharya[3]

[1]*Laboratory of Physics, Helsinki University of Technology, P.O. Box 1100, FIN-02015 TKK, Espoo, Finland*
[2]*Department of Physics, Box 1843, Brown University, Providence, Rhode Island 02912-1843, USA*
[3]*Department of Physics, University of Central Florida, Orlando, Florida 32816-2385, USA*

We investigate the influence of polymer-pore interactions on the translocation dynamics using Langevin dynamics simulations. An attractive interaction can greatly improve the translocation probability. At the same time, it also increases the translocation time slowly for a weak attraction while an exponential dependence is observed for a strong attraction. For fixed driving force and chain length the histogram of translocation time has a transition from Gaussian distribution to long-tailed distribution with increasing attraction. Under a weak driving force and a strong attractive force, both the translocation time and the residence time in the pore show a nonmonotonic behavior as a function of the chain length. Our simulations results are in good agreement with recent experimental data.

The transport of a polymer through a nanopore plays a critical role in numerous biological processes, such as DNA and RNA translocation across nuclear pores, protein transport through membrane channels, and virus injection. For a polymer threading through a nanopore, loss of available configurations due to the geometric constriction leads to an effective entropic barrier. Kasianowicz *et al.* [1] demonstrated that an electric field can drive single-stranded DNA and RNA molecules through the water-filled α-hemolysin channel and that the passage of each molecule is signaled by a blockade in the channel current. These observations can directly be used to characterize the polymer length. Because of various potential technological applications [1,2], such as rapid DNA sequencing, gene therapy and controlled drug delivery, the polymer translocation has become a subject of intensive experimental [3–10] and theoretical [10–24] studies.

As to translocation, one of the basic questions concerns the dependence of the translocation time τ on the system parameters such as the polymer chain length N [5,6,10–13,16–24], sequence and secondary structure [3,4,6,22], pore length L and pore width W [19], driving force F [5–8,17,20,21,23,24], and polymer-pore interaction [4,6,9,13,23].

In a recent experiment, [4,6] striking differences were found for the translocation time distribution of polydeoxyadenylic acid (poly(dA)$_{100}$) and polydeoxycytidylic acid (poly(dC)$_{100}$) DNA molecules. The origin of the different behavior was attributed to a stronger attractive interaction of poly(dA) with the pore. Also, recently Krasilnikov *et al.* [9] have investigated the dynamics of single poly (ethylene glycol) (PEG) molecules in the α-hemolysin channel in the limit of a strong attractive polymer-pore attraction. The result for the residence time in the channel shows a novel nonmonotonic behavior as a function of the molecular weight.

On the theoretical front, not only the quantitative but also the qualitative picture of the polymer-nanopore interactions is still elusive. Based on a Smoluchowski equation with a phenomenological microscopic potential to describe the polymer-pore interactions, Lubensky and Nelson [13] captured the main ingredients of the translocation process. However, when comparing with experiments, their model is not sufficient. Numerically, Tian and Smith [23] found that attraction facilitates the translocation process by shortening the translocation time, which contradicts experimental findings [4,6].

To this end, in this Letter we use Langevin dynamics to investigate the influence of polymer-pore interactions on translocation. In our numerical simulations, the polymer chains are modeled as bead-spring chains of Lennard-Jones (LJ) particles with the finite extension nonlinear elastic (FENE) potential. Excluded volume interaction between monomers is modeled by a short range repulsive LJ potential: $U_{LJ}(r) = 4\varepsilon[(\frac{\sigma}{r})^{12} - (\frac{\sigma}{r})^6] + \varepsilon$ for $r \leq 2^{1/6}\sigma$ and 0 for $r > 2^{1/6}\sigma$. Here, σ is the diameter of a monomer, and ε is the depth of the potential. The connectivity between neighboring monomers is modeled as a FENE spring with $U_{FENE}(r) = -\frac{1}{2}kR_0^2 \ln(1 - r^2/R_0^2)$, where r is the distance between consecutive monomers, k is the spring constant and R_0 is the maximum allowed separation between connected monomers.

We consider a 2D geometry as shown in Fig. 1, where the wall in the y direction is described as stationary particles within a distance σ from each other. The pore of length L and width W in the center of the wall is composed of stationary black particles. Between all monomer-wall particle pairs, there exist the same short range repulsive LJ interaction as described above. The pore-monomer interaction is modeled by a LJ potential with a cutoff of 2.5σ and interaction strength ε_{pm}. This interaction can be either attractive or repulsive depending on the position of the monomer from the pore particles. We have also performed numerical calculation for the case of a pure short range repulsive LJ potential for the pore-monomer interaction.
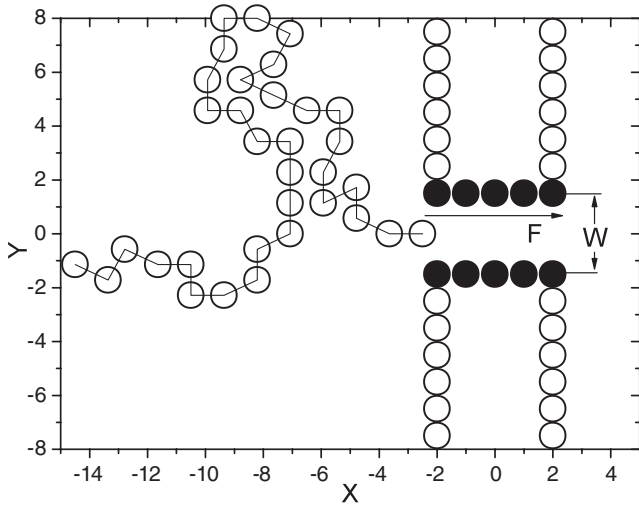
148102-1

FIG. 1.   A schematic representation of the system. The pore
length $L = 5$ and the pore width $W = 3$ (See text for units).

As expected, the results for the long range LJ pore-
monomer interaction approaches that for the pure repulsive
pore-monomer interaction in the limit $\varepsilon_{pm} \rightarrow 0$. In the
Langevin dynamics simulation, each monomer is subjected
to conservative, frictional, and random forces, respectively,
with [25] $m\ddot{\mathbf{r}}_i = -\nabla(U_{LJ} + U_{FENE}) + \mathbf{F}_{ext} - \xi\mathbf{v}_i + \mathbf{F}_i^R$,
where m is the monomer's mass, ξ is the friction coeffi-
cient, $\mathbf{v}_i$ is the monomer's velocity, and $\mathbf{F}_i^R$ is the random
force which satisfies the fluctuation-dissipation theorem.
The external force is expressed as $\mathbf{F}_{ext} = F\hat{x}$, where F is
the external force strength exerted on the monomers in the
pore, and $\hat{x}$ is a unit vector in the direction along the pore
axis.

In the present work, we use the LJ parameters ε and σ
and the monomer mass m to fix the energy, length and mass
scales, respectively. The time scale is then given by $t_{LJ} = (m\sigma^2/\varepsilon)^{1/2}$ The dimensionless parameters in our simula-
tions are $R_0 = 2$, $k/m = 7$, $k_B T = 1.2$, and $\xi/m = 0.7$.
For the pore, we set $L = 5$ unless otherwise stated. A
choice of $W = 3$ ensures that the polymer encounters an
attractive force inside the pore. We have checked that a
choice of $W = 4$ yields similar results. The driving force F
is set between 0.5 and 2.0, which correspond to the range of
voltages used in the experiments [1,5]. The Langevin
equation is integrated in time by a method described by
Ermak and Buckholz [26] in 2D. Initially, the first mono-
mer of the chain is placed in the entrance of the pore, while
the remaining monomers are under thermal collisions de-
scribed by the Langevin thermostat to obtain an equilib-
rium configuration. The translocation time is defined as the
time interval between the entrance of the first segment into
the pore and the exit of the last segment. Typically, we
average our data over 2000 independent runs.

The translocation probability, P_{trans}, is calculated as the
fraction of runs leading to successful translocation at given
conditions. Figure 2(a) shows P_{trans} as a function of ε_{pm} for
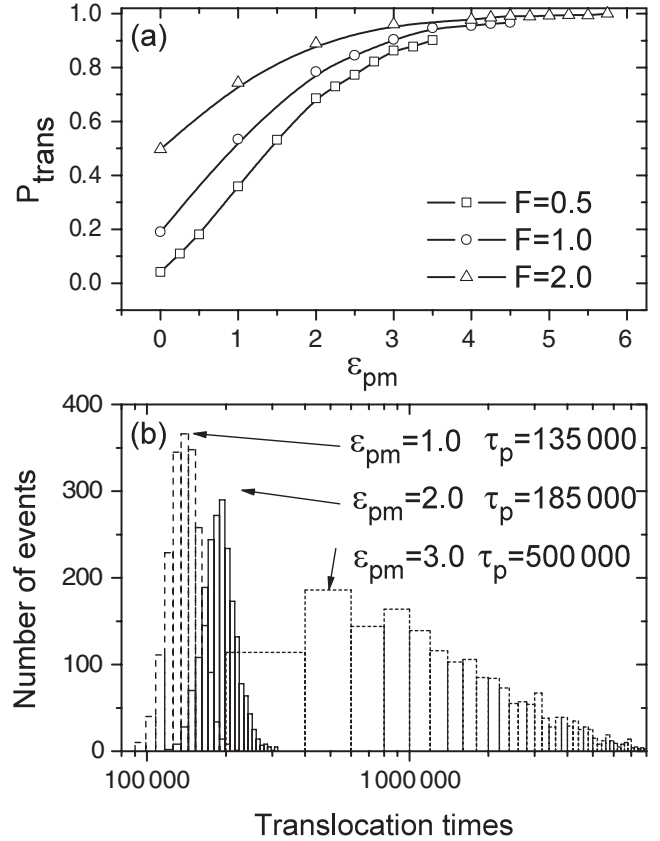$N = 128$ under different driving forces. Specifically, the

FIG. 2.   (a) The translocation probability as a function of the
attractive strength for different driving forces. (b) The distribu-
tion of translocation time for different attractive strengths under
the driving force $F = 0.5$. The chain length $N = 128$. The data
point at $\varepsilon_{pm} = 0$ corresponds to a pure repulsive pore-monomer
interaction.

numerical results clearly show two different regimes. With
increasing ε_{pm}, P_{trans} increases rapidly first, and then
slowly approaches saturation at larger ε_{pm}. It is known
that attractive interaction with the channel can facilitate
the translocation of metabolite molecule across cellular
and organelle membranes [27]. Here, our results show
that polymer translocation through the attractive nanopore
shares the same character.

Experimentally, Meller et al. [4,6] have investigated the
translocation of homopolynucleotides of different bases:
poly(dA)$_{100}$ and poly(dC)$_{100}$. The translocation time dis-
tributions in both cases are well approximated by fast-
growing Gaussian for translocation time lower than the
most probable value τ_p and falling exponentials for trans-
location time larger than τ_p. The decay time scale for
poly(dA) is found to be much longer than poly(dC), by a
factor of $\sim$7. There exists also a large difference between
the value of τ_p for the two, corresponding to 1.2 μs/base
for poly(dC), and 3.3 μs/base for poly(dA). These differ-
ences have been attributed to the base specific nucleotide-
pore interactions, with the adenines having a stronger

attractive interaction with the pore as compared with cytosines.

In our numerical results, we have found that indeed for $\varepsilon_{pm} = 2$ and 3, the attractive potential has a marked impact on the shape of the histogram of the translocation time as shown in Fig. 2(b). The shape of the histogram changes from a nearly Gaussian below the most probable value to a long exponential tail. The value of τ_p as well as the characteristic decaying time scale increases with ε_{pm}. These findings are in excellent agreement with the experimental observation of Meller *et al.* [4,6], and provide further support that the base specific interaction with the pore plays a pivotal role in the translocation dynamics of single-stranded DNA and RNA molecules.

Figure 3 shows the calculated τF as a function of ε_{pm} for $N = 128$ under different driving forces. Initially, τ increases very slowly with increasing ε_{pm}. Then, it crosses over to a different regime and increases sharply to the asymptotic behavior $\tau F \sim e^{L/k_B T}$. The crossover threshold value of ε_{pm} increases with increasing F. Surprisingly, previous numerical work [23] failed to capture the essential feature that the translocation time increases with increasing attractive base-pore interaction.

An important element of our analysis is the fact that the translocation time can be written as $\tau \sim \tau_1 + \tau_2 + \tau_3$, where τ_1, τ_2, and τ_3 correspond to initial filling of the pore, transfer of the DNA from the *cis* side to the *trans* side, and finally the emptying of the pore, respectively. In the presence of the attractive pore-monomer interaction and driving force across the pore, $\tau_1 \ll \tau_2$, τ_3 while τ_2 increases monotonically with N. For strong attraction and intermediate values of N, τ is determined mainly by τ_3 related to the emptying of the pore. This process involves a free energy difference of $\Delta\tilde{F} = L[\varepsilon_{pm} - F/2 - f(N)]$ between the final and the initial state. The term $f(N)$ here

accounts for the entropic driving force which should kick in at larger values of N and eventually saturate for very long polymers. For the region of weak attraction below the threshold, $\Delta\tilde{F} < 0$ and the translocation time depends weakly on ε_{pm}. Above the threshold when $\Delta\tilde{F} > 0$, the process is activated with a barrier $\sim \Delta\tilde{F}$ and increases rapidly with increasing strength of attraction ε_{pm}. This accounts for the observed crossover behavior of τ as a function of ε_{pm}. In the weak attraction nonactivated region, the overall τ is determined mainly by τ_2 and its dependence on the driving force scales as F^{-1}, which comes from the velocity dependence on F. However, once one enters the activated region, the force F also influences the activation barrier besides affecting the prefactor and τ drops off with increasing F much faster than the simple F^{-1} behavior.

For $F = 0.5$ and a pure repulsive pore-monomer interaction, we have shown in our earlier work [20,21] that $\tau \sim N^{2\nu}$ for relatively short chains and crosses over to $\tau \sim N^{1+\nu}$ for longer chains as shown in Fig. 4, where the Flory exponent $\nu = 0.75$ in two dimensions [28], and the crossover length $N_c \sim 200$. The scaling behavior for attractive interaction strength $\varepsilon_{pm} = 1$ is very similar to the pure repulsive case. For $\varepsilon_{pm} = 2$, we found that $N_c \sim 310$. For stronger attractive strength $\varepsilon_{pm} = 3$, only $\tau \sim N^{2\nu}$ is observed for the N values studied under $F = 1$ and $F = 2$, with no indication of crossover behavior as shown in the inset of Fig. 4.

Under a strong attractive force with $\varepsilon_{pm} = 3$ and a weak driving force $F = 0.5$, the translocation time τ has a qualitatively different dependence on N as compared with the pure repulsive or weak attractive pore interaction. It has a novel nonmonotonic behavior with a rapid increase to a maximum at $N \sim 14$, followed by a decrease for $14 < N < 32$ and an increases again for $N > 32$ as shown in
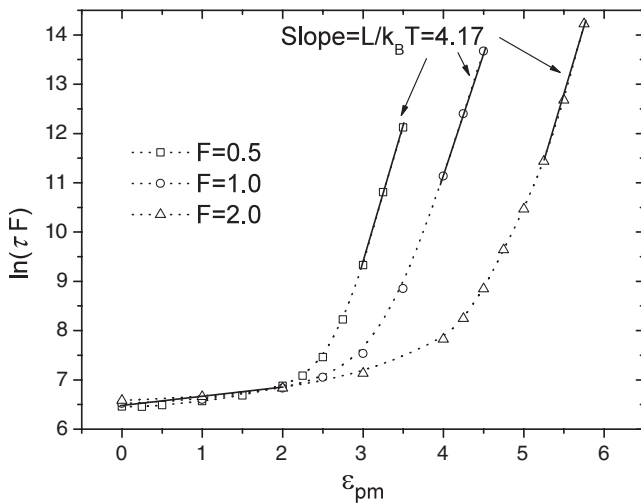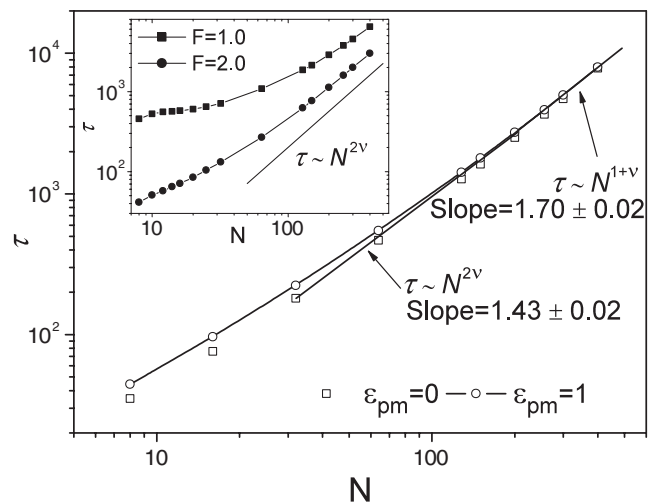
FIG. 3. Translocation time as a function of the attractive strength for different driving forces. The chain length $N = 128$. Here, $\varepsilon_{pm} = 0$ corresponds to a pure repulsive pore-monomer interaction.

FIG. 4. Translocation time as a function of the chain length for $\varepsilon_{pm} = 0$ and $\varepsilon_{pm} = 1$ with $F = 0.5$. The insert shows results for $\varepsilon_{pm} = 3$ with $F = 1.0$ and $F = 2.0$.

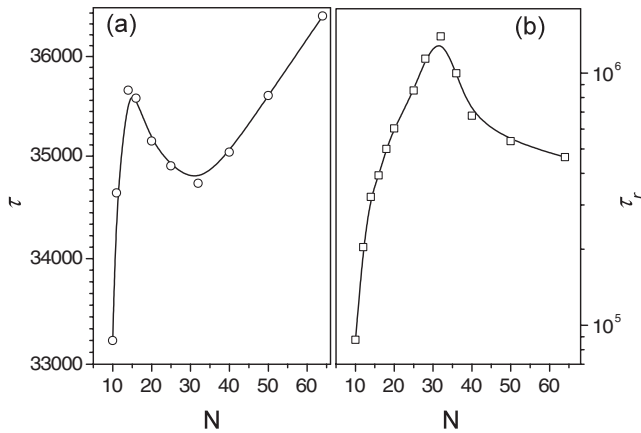FIG. 5.   (a) Translocation time τ as a function of the chain
length for $\varepsilon_{\mathrm{pm}} = 3$ and $F = 0.5$. (b) Residence time τ_r as a
function of the chain length for $\varepsilon_{\mathrm{pm}} = 3$ and $F = 0$.

Fig. 5(a). This can be understood by considering the differ-
ent N dependence of τ_1, τ_2, and τ_3 in the strong attraction
limit. For small and intermediate values of N, τ is domi-
nated by τ_3. Here the entropic factor $f(N)$ in the barrier for
τ_3 fights against the simple power law increase in the
prefactor accounting for the number of monomers needed
to cross the pore. This leads to an initial increase of τ to a
maximum value followed by a subsequent decrease.
Eventually, for larger N, the τ_2 process (which approaches
$N^{2\nu}$ asymptotically) takes over, leading to the increase of τ
with increasing N again.

For this case, we found that there is about 20% of the
total translocation processes in which the polymer enters
and reexits the *cis* side of the pore. It is useful to define an
additional residence time τ_r as the weighted sum of the
translocation time and the return time which corresponds to
the experimentally measured blockage time. For the case
with no external driving force, the translocation probability
is very small and the residence time is almost all due to
return events. We have calculated the residence time τ_r for
$F = 0$ and $\varepsilon_{\mathrm{pm}} = 3$ and the result is shown in Fig. 5(b).
The N dependence here is again nonmonotonic similar
to the translocation time for $F = 0.5$ except for the absence
of the eventual increase at the large N limit, due to the
absence of the τ_2 contribution for the return process. Our
numerical result of τ_r for $F = 0$ is in good agreement
with recent experimental data of Krasilnikov *et al.* [9] in
which the residence time of neutral PEG molecule in
α-Hemolysin pore was measured.

To summarize, we have investigated the influence of
attractive polymer-pore interactions on the translocation
dynamics via numerical simulation studies of a simple
course grained model. Our results are in good agreement
with recent experimental data for driven translocation of
poly(dA) and poly(dC) molecules, and for the blockage
time study of poly(ethylene glycol) molecule through
α-hemolysin pore. They clearly demonstrate the important
role of polymer-pore interaction factor in the translocation
dynamics.

*Author to whom all correspondence should be addressed.
luokaifu@yahoo.com
 [1] J. J. Kasianowicz, E. Brandin, D. Branton, and D. W.
     Deamer, Proc. Natl. Acad. Sci. U.S.A. **93**, 13 770 (1996).
 [2] A. Meller, J. Phys. Condens. Matter **15**, R581 (2003).
 [3] M. Akeson, D. Branton, J. J. Kasianowicz, E. Brandin, and
     D. W. Deamer, Biophys. J. **77**, 3227 (1999).
 [4] A. Meller, L. Nivon, E. Brandin, J. A. Golovchenko, and
     D. Branton, Proc. Natl. Acad. Sci. U.S.A. **97**, 1079 (2000).
 [5] A. Meller, L. Nivon, and D. Branton, Phys. Rev. Lett. **86**,
     3435 (2001).
 [6] A. Meller and D. Branton, Electrophoresis **23**, 2583
     (2002).
 [7] S. E. Henrickson, M. Misakian, B. Robertson, and J. J.
     Kasianowicz, Phys. Rev. Lett. **85**, 3057 (2000).
 [8] A. F. Sauer-Budge, J. A. Nyamwanda, D. K. Lubensky,
     and D. Branton, Phys. Rev. Lett. **90**, 238101 (2003).
 [9] O. V. Krasilnikov, C. G. Rodrigues, and S. M. Bezrukov,
     Phys. Rev. Lett. **97**, 018301 (2006).
[10] A. J. Storm, C. Storm, J. Chen, H. Zandbergen, J.-F.
     Joanny, and C. Dekker, Nano Lett. **5**, 1193 (2005).
[11] W. Sung and P. J. Park, Phys. Rev. Lett. **77**, 783 (1996).
[12] M. Muthukumar, J. Chem. Phys. **111**, 10 371 (1999).
[13] D. K. Lubensky and D. R. Nelson, Biophys. J. **77**, 1824
     (1999).
[14] R. Metzler and J. Klafter, Biophys. J. **85**, 2776 (2003).
[15] T. Ambjornsson, M. A. Lomholt, and R. Metzler, J. Phys.
     Condens. Matter **17**, S3945 (2005).
[16] J. Chuang, Y. Kantor, and M. Kardar, Phys. Rev. E **65**,
     011802 (2001).
[17] Y. Kantor and M. Kardar, Phys. Rev. E **69**, 021806 (2004).
[18] A. Milchev, K. Binder, and A. Bhattacharya, J. Chem.
     Phys. **121**, 6042 (2004).
[19] K. F. Luo, T. Ala-Nissila, and S. C. Ying, J. Chem. Phys.
     124, 034714 (2006).
[20] K. F. Luo, I. Huopaniemi, T. Ala-Nissila, and S. C. Ying,
     J. Chem. Phys. **124**, 114704 (2006).
[21] I. Huopaniemi, K. F. Luo, T. Ala-Nissila, and S. C. Ying,
     J. Chem. Phys. **125**, 124901 (2006); Phys. Rev. E **75**,
     061912 (2007).
[22] K. F. Luo, T. Ala-Nissila, S. C. Ying, and A. Bhattacharya,
     J. Chem. Phys. **126**, 145101 (2007).
[23] P. Tian and G. D. Smith, J. Chem. Phys. **119**, 11 475
     (2003).
[24] S. Matysiak, A. Montesi, M. Pasquali, A. B. Kolomeisky,
     and C. Clementi, Phys. Rev. Lett. **96**, 118103 (2006).
[25] M. P. Allen and D. J. Tildesley, *Computer Simulation of
     Liquids* (Oxford University, New York, 1987).
[26] D. L. Ermak and H. Buckholz, J. Comput. Phys. **35**, 169
     (1980).
[27] A. M. Berezhkovskii, M. A. Pustovoit, and S. M.
     Bezrukov, J. Chem. Phys. **116**, 9952 (2002); **119**, 3943
     (2003).
[28] P. G. de Gennes, *Scaling Concepts in Polymer Physics*
     (Cornell University, Ithaca, NY, 1979).